Redox-controlled molecular permeability of composite-wall microcapsules

YUJIE MA[1], WEN-FEI DONG[2], MARK A. HEMPENIUS[1], HELMUTH MÖHWALD[2] AND G. JULIUS VANCSO[1]*

[1]Department of Materials Science and Technology of Polymers, MESA+ Research Institute for Nanotechnology, University of Twente, PO Box 217, NL-7500 AE Enschede, The Netherlands

[2]Max Planck Institute of Colloids and Interfaces, Golm/Potsdam, D-14476, Germany

*e-mail: g.j.vancso@tnw.utwente.nl

Published online: 20 August 2006; doi:10.1038/nmat1716

Many smart materials in bioengineering, nanotechnology and medicine allow the storage and release of encapsulated drugs on demand at a specific location by an external stimulus. Owing to their versatility in material selection, polyelectrolyte multilayers are very promising systems in the development of microencapsulation technologies with permeation control[1–4] governed by variations in the environmental conditions[5–8]. Here, organometallic polyelectrolyte multilayer capsules, composed of polyanions and polycations of poly(ferrocenylsilane) (PFS), are introduced. Their preparation involved layer-by-layer self-assembly onto colloidal templates followed by core removal. PFS polyelectrolytes feature redox-active ferrocene units in the main chain. Incorporation of PFS into the capsule walls allowed us to explore the effects of a new stimulus, that is, changing the redox state[9,10], on capsule wall permeability. The permeability of these capsules could be sensitively tuned via chemical oxidation, resulting in a fast capsule expansion accompanied by a drastic permeability increase in response to a very small trigger. The substantial swelling could be suppressed by the application of an additional coating bearing common redox-inert species of poly(styrene sulfonate) (PSS^-) and poly(allylamine hydrochloride) (PAH^+) on the outer wall of the capsules. Hence, we obtained a unique capsule system with redox-controlled permeability and swellability with a high application potential in materials as well as in bioscience.

'Smart' polymers can recognize a stimulus as a signal and then significantly alter for instance their chain conformation in response to small changes in the environmental conditions[11]. Molecular structures that are composed of such materials, with the ability to be triggered to contract or expand in a controlled fashion, have great application potential in numerous fields, including nanotechnology, biochemistry, organic and physical chemistry, and materials science[12]. Conventional, organic polyelectrolyte-based microcapsules have limitations in some significant applications due to their slow response to trace amounts of trigger and restrictions on the choice of stimuli. Electrochemical stimuli are very promising, because (1) the redox potential near an organ where a pharmaceutical drug should be released may differ from other locations in the body, and (2) a corrosion pit may self-anneal due to the release of an inhibitor caused by a change in the local potential. However, this requires the construction of capsules with redox-active compounds. Poly(ferrocenylsilanes) (PFS), composed of organometallic units in the main chain, belong to the class of stimulus-responsive materials. Owing to the ferrocene-bearing repeating units of the polymer, PFS can be reversibly oxidized and reduced by chemical[13–15] as well as electrochemical means[16,17]. Atomic force microscopy (AFM)-based single-molecule force spectroscopy measurements on PFS single chains[9,10,18] showed a significantly increased Kuhn length and segment elasticity after oxidation, which is direct proof of redox-induced changes of the torsional potential energy landscape.

Water soluble PFS polycations and polyanions[19–22], belonging to the rare class of main-chain organometallic polyelectrolytes, have recently been reported by us and others. These compounds all bear certain charges on the polymer side groups so that they can be used in the electrostatic layer-by-layer (LBL) self-assembly[23] process to form multilayer films and hollow capsules[24] with defined structure and function due to the molecular characteristics of the organometallic main chain.

The organometallic polyelectrolyte multilayer capsules reported here are based on the water-soluble PFS polyanion **1** and polycation **2**. As demonstrated in Fig. 1, PFS capsules were fabricated by the electrostatic LBL assembly of these polyelectrolytes onto colloidal templates. These templates were removed at the completion of the assembly. Before studying the encapsulation and release, the capsule structures were characterized in detail. The electrostatic LBL assembly process was followed by electrophoretic mobility measurements. Figure 2a summarizes the changes in zeta(ζ)-potential recorded on layer deposition for polyanion/polycation pairs (in the sequence of $(PSS^-/PAH^+)_2(PFS^-/PFS^+)_3$) on melamine formaldehyde (MF) cores. The alternation of the ζ-potential between positive and negative values indicated the successful charge reversal of the particle surfaces during the LBL sequential deposition[25]. After removing the MF cores using HCl (pH = 1.0) and subsequently

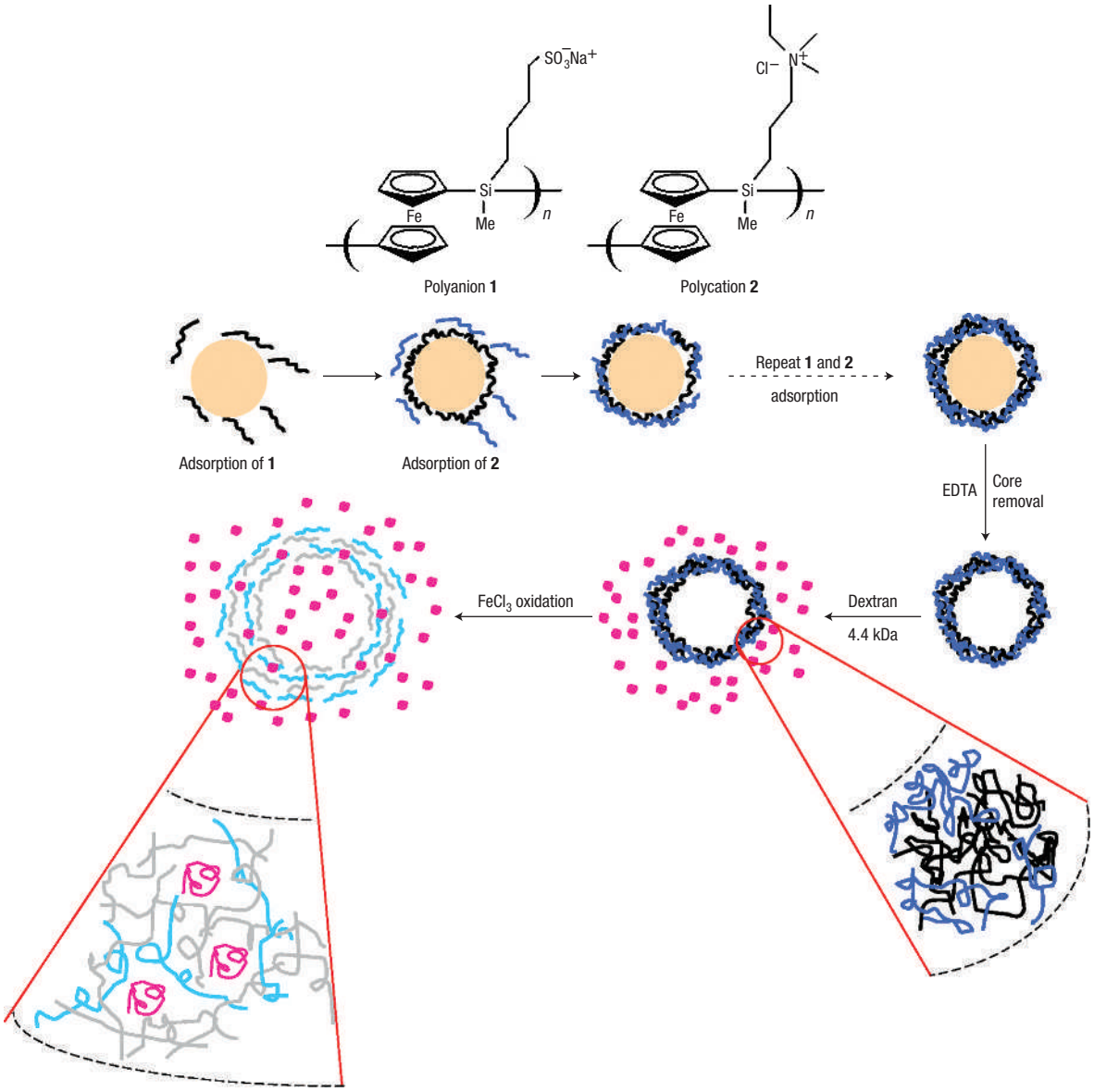

Figure 1 Schematic diagrams of the organometallic multilayer capsule formation and permeability control. Polyanion **1** (black lines) and polycation **2** (blue lines) were used in the electrostatic self-assembly onto curved substrates followed by core removal. The permeability of the obtained capsules could be tuned via chemical oxidation for example, by $FeCl_3$. Red bundles represent dextran. The varying colours of the polymer chains in the bottom left represent their different oxidational/conformational states.

carrying out several rinsing steps, ultraviolet/visible measurements were carried out on the aqueous dispersion of the obtained capsules ($(PSS^-/PAH^+)_3(PFS^-/PFS^+)_2$ capsule wall structure). As shown in Fig. 2b, the absorbance characteristic of PFS was observed as an intense ligand-to-metal charge-transfer transition at 216 nm, in accordance with previous results on planar PFS polyelectrolyte multilayer films[19,22]. In addition, the slowly precipitated capsules were yellow, indicating the presence of ferrocene-containing material in the capsule wall.

Complementary to the MF cores, more-stable microcapsules, solely composed of PFS polyanions and polycations with a better-defined integrity, were fabricated in high yield using manganese carbonate ($MnCO_3$) templates. Metal carbonate crystals that can be removed by ethylenediaminetetraacetic acid (EDTA) solutions have been intensively used in recent years due to their suitability in the fabrication of clean capsules, dissolution in mild conditions and relative ease of synthesis[26,27]. Figure 2c shows an example of a dried capsule with four bilayers of PFS polyanion/polycation. An average bilayer (PFS^-/PFS^+) thickness of 6.0 ± 0.3 nm for adsorption from 0.5 M NaCl was calculated. This value was larger than the typical bilayer thicknesses (~4.5 nm) obtained on planar (silicon or gold) substrates under the same adsorption conditions. A possible explanation for this variation in film thickness may be related to the dependence of multilayer film growth on the characteristics of the templating materials, for example, on surface charge density[28]. The surface of the collapsed capsules, as shown in AFM images, exhibited a roughness (r.m.s., in an area of $3 \times 3\ \mu m^2$) of ~5 nm, which was significantly larger than the respective r.m.s. values obtained for multilayer films on planar substrates, which were in the sub-nanometre range.

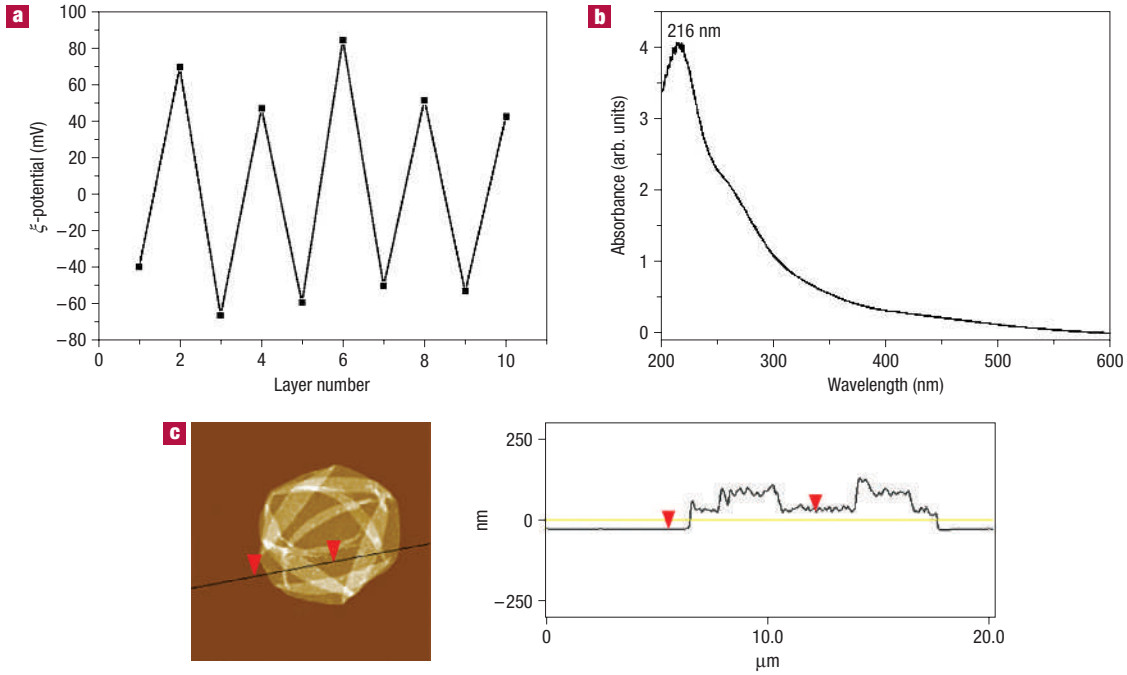

Figure 2 Characterization of PFS multilayer microcapsules. a, Zeta-potential measurements following the LBL deposition process of PFS polyions on MF cores. **b**, Ultraviolet/visible spectrum of the aqueous dispersion of $(PSS^{-}/PAH^{+})_2(PFS^{-}/PFS^{+})_3$ capsules. The strong absorption peak at $\lambda = 216$ nm is characteristic of PFS. **c**, A collapsed PFS capsule (four bilayers of (PFS^{-}/PFS^{+})) imaged by tapping-mode AFM in the dry state; the AFM thickness of the capsules was measured by the difference in the heights corresponding to the arrows.

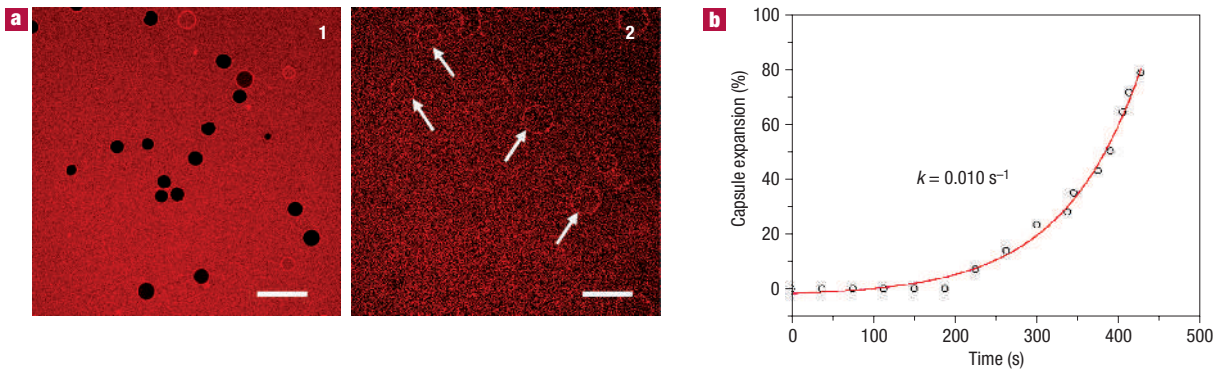

Figure 3 Redox-responsive permeability accompanied by expansion of PFS capsules. a, Confocal fluorescence micrographs of a capsule solution containing 4.4-kdalton TRITC-labelled dextran before (1) and after (2) $FeCl_3$ oxidation. The arrows indicate expanded capsules. Scale bar = 40 μm. **b**, PFS capsule expansion with time in the final oxidized states. The circles represent the experimental data and the red line is an exponential fit, which gives a first-order expansion rate constant of $k = 0.010\ s^{-1}$ for the example shown.

The unique chemical constitution of these capsules ensures their peculiar redox-responsive permeability (Fig. 1). To study the response of our PFS capsules to redox stimuli, ferric chloride ($FeCl_3$) was chosen as the oxidant due to its effectiveness in oxidizing PFS[13] and its water solubility under slightly acidic conditions. Tetramethylrhodamine isothiocyanate (TRITC)-labelled dextran (4.4 kdalton) was used as a fluorescent probe to monitor permeability. PFS capsules that were originally impermeable to these molecules were mixed on-site with an aqueous $FeCl_3$ solution (1 mM, pH = 4, tuned by HCl) during *in situ* confocal laser scanning microscopy (CLSM) imaging. On exposure to Fe^{3+} ions originating from $FeCl_3$, the PFS capsules exhibited a continuous expansion accompanied by an increasing permeability of the capsules as shown by fluorescence imaging. Figure 3a shows the CLSM images of PFS capsules (with 6 bilayers) before and after oxidation. Image 2 in Fig. 3a reveals that the oxidized capsules were completely permeable to 4.4-kdalton dextran molecules, as it was no longer possible to differentiate the fluorescence intensity from outside and inside the capsules. Following the exposure to $FeCl_3$, a substantial change in the capsule

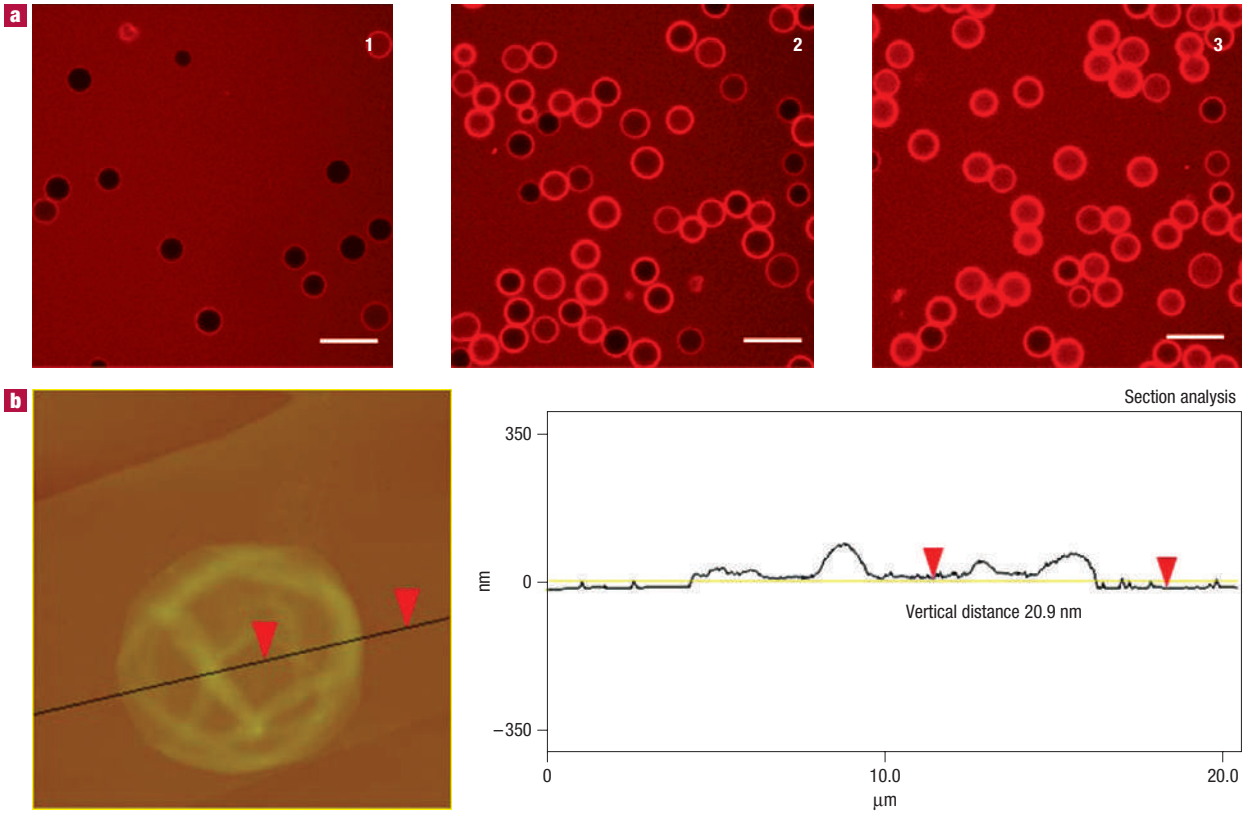

Figure 4 Redox-responsive permeability of multilayer capsules with organometallic–organic composite-wall structures. a, Local oxidation of $(PFS^{-}/PFS^{+})_5(PSS^{-}/PAH^{+})_1$ microcapsules by $FeCl_3$ (1 mM, pH = 4) monitored by CLSM. Capsules that are originally impermeable (1) to 4.4-kdalton dextran molecules show partial permeability (2) in the early stage of oxidation (10 min) and almost complete permeability (3) after oxidation for more than 1 h. Scale bar = 20 μm. **b**, Tapping-mode AFM height image of a $(PFS^{-}/PFS^{+})_5(PSS^{-}/PAH^{+})_1$ capsule after oxidation for over 2 h by $FeCl_3$ (1 mM, pH = 4). The integrity of the capsules has been preserved.

size accompanied the onset of permeability, as observed for the oxidized capsules in Fig. 3a. It should be noted that permeability was statistically defined and the overall permeability referred to a situation where ≥90% capsules exhibited the same quality.

Expansion of the capsules proceeds in a continuous manner until their final disappearance. The process of expansion and disintegration was monitored as a function of time to describe the kinetics of the capsule swelling under these conditions. The oxidation-induced expansion sets in following an induction period of about 15 min at room temperature. The induction period is a result of a slow diffusion of the Fe^{3+} ions to the location of the capsules and to the capsule interior, and is thus not a consequence of a slow oxidation reaction (see the Supplementary Information). After the induction period, data were collected on the mean diameter values of the capsules from the onset of adding $FeCl_3$ until the final disappearance of the capsules. The continuous capsule expansion could actually be stopped by adding effective PFS reducing agents, for example, dithiothreitol, during the oxidation process. The degree of capsule expansion was calculated (averaged over a population of about 20 capsules) as:

$$\text{capsule expansion}\ (\%) = \frac{\overline{d_t - d_0}}{d_0} \times 100\%,$$

where d is the diameter of the capsules observed by CLSM, with subscripts 0 and t denoting values before and at 't', respectively.

Figure 3b summarizes the expansion data as a function of time. The circles in Fig. 3b represent the experimental data that were fitted by a simple exponential growth curve as shown by the red line. The data indicated that the capsules expanded in an accelerated manner towards the final disintegration, following kinetics similar to a first-order reaction, where the rate law can be described as:

$$\frac{A}{A_0} - 1 = e^{kt}$$

where k is the rate constant. A fit of the data resulted in a typical k value of $0.010\,s^{-1}$ in the present case, and this value was found to strongly depend on the concentration of the oxidant. Our study on the local oxidation of $(PFS^{-}/PFS^{+})_5$ capsules showed that when the concentration of the $FeCl_3$ solutions decreased from 3 to 1 mM, the duration of complete capsule disintegration increased from 2 to 15 min. These times are more than one order of magnitude shorter than those measured for main-chain scission[29], and it was therefore concluded that they were determined by the build-up of charges inside the films.

The observed oxidation-induced capsule permeability change and disintegration are peculiar, especially because a very small trigger ($FeCl_3$ with a sub-mM concentration) is sufficient to cause the change. This expansion was interpreted as a result of several factors. First, oxidation of the ferrocenyl groups on the polymer causes the amount of positive charges along the main chain to

increase. Thus, in a multilayered structure containing the same polymer backbone, electrostatic repulsion due to the excess positive charge on the chains would increase the distance between like-charged segments, that is, an expansion both along the chain and in the multilayer growth direction would be favoured. As mentioned, we have shown previously that a stiffening (that is, an increase in the Kuhn segment length and segment elasticity) accompanies oxidation[9,10]. This effect may also contribute to increase the average pore size and enhance the permeability accordingly. During oxidation, the original PFS^- and PFS^+ both pick up additional positive charges; this in turn modifies the overall charge density on the polycations and polyanions in opposite directions. Polycations become more highly charged on oxidation, whereas polyanions become neutral. In essence, because the electrostatic neutrality in the as-prepared LBL structures is lost, we expect complete disintegration of the capsules after full oxidation.

To maintain the integrity of the capsules, and at the same time effectively change the capsule permeability, composite-wall capsules with PFS^-/PFS^+ polyion pairs as inner layers and redox-insensitive polyelectrolyte pairs (PSS^-/PAH^+) in the outer layers were fabricated. Examples of CLSM micrographs of capsules composed of $(PFS^-/PFS^+)_5(PSS^-/PAH^+)_1$ are shown in Fig. 4a. These capsules were robust and essentially impermeable to 4.4-kdalton dextran molecules in the neutral state. After adding $FeCl_3$ (1 mM) solution, the capsules started to become permeable, as indicated by the strong increase in the fluorescence intensity in the capsule interior (image 2). During the course of the oxidation process of PFS, an almost complete permeability of all capsules was observed (Fig. 4a, image 3). CLSM images also exhibited a gradual accumulation of dye molecules in the capsule wall (see also Fig. 1). Similar dye accumulation has been reported previously[4]. The capsule integrity was preserved, as shown in Fig. 4b. However, the double wall thickness of the capsules decreased from 69 ± 3 nm before oxidation to 22 ± 3 nm after oxidation for over 2 h, indicating some loss of material related to maintaining charge neutrality. Neither CLSM nor AFM measurements showed any measurable capsule size change before and following oxidation.

In addition to varying the concentration of oxidants, the rate of permeability change could also be tuned by the number of PSS^-/PAH^+ bilayers on the outer wall of the capsules. Increasing the number of outer layers slowed the permeability change of the capsules. Obviously the capping redox-inert bilayers acted as 'blocking' layers on the capsule surface. When varying the number of capping PSS^-/PAH^+ bilayers from $n = 1$–3 on the same $(PFS^-/PFS^+)_5$ inner-layer structure and using the same oxidant concentration, the recorded timescale for more than 80% of the impermeable capsules to become permeable increased from 1 to 6 h.

MATERIALS AND METHODS

The detailed synthesis of the PFS polyions **1** and **2** (Fig. 1) has been described elsewhere[21]. PSS (molecular mass: ~70 kdalton), PAH (molecular mass: ~70 kdalton), and TRITC-labelled dextran (TRITC-dextran, molecular mass: ~4.4 kdalton) were obtained from Aldrich and used as received. Manganese carbonate particles (10 μm) were prepared according to reported methods[26]. MF particles (5 μm) were purchased from Microparticles GmbH.

FABRICATION OF POLYELECTROLYTE MULTILAYER CAPSULES

Alternating adsorption of polyelectrolytes (PFS, 1 mg ml^{-1}; PSS/PAH, 2 mg ml^{-1}) onto the colloidal microparticles (~10% w/w in suspension) was carried out in 0.5 M NaCl solution for 10 min followed by centrifugation (1,500 r.p.m., 1 min) and three MilliQ washing/centrifugation steps. Depending on the composition, HCl (MF) or EDTA ($MnCO_3$) was used to remove the core material.

CLSM

CLSM images were obtained with either a Leica TCS NT (×100 or ×40 oil immersion objective) or Zeiss LSM 510 (×63 oil immersion objective) confocal scanning system. Equal volumes of capsule suspension and TRITC-dextran (2 mg ml^{-1}) were mixed before observation. On-site oxidized samples were monitored by adding another equal volume of oxidant solution and carrying out a continuous scan under the same spot in focus.

AFM

Capsule samples were prepared by applying a droplet of capsule suspension on a freshly cleaved mica surface and subsequent dry-blowing. AFM images were taken in tapping mode using silicon cantilevers (Nanosensors) on a NanoScope IIIa multimode AFM (Veeco-Digital Instruments) at room temperature, in air.

ZETA-POTENTIAL MEASUREMENTS

The ζ-potential of the microcapsules was measured in water using a Zetasizer Nanoinstrument Nano Z setup. Each value was averaged from 5 parallel measurements.

ULTRAVIOLET/VISIBLE SPECTROSCOPY

Ultraviolet/visible spectra were recorded using a Cary 300 UV/vis spectrophotometer.

Received 28 February 2006; accepted 24 July 2006; published 20 August 2006.

References

1. Dähne, L., Leporatti, S., Donath, E. & Möhwald, H. Fabrication of micro reaction cages with tailored properties. *J. Am. Chem. Soc.* **123,** 5431–5436 (2001).
2. Lvov, Y., Antipov, A. A., Mamedov, A., Möhwald, H. & Sukhorukov, G. B. Urease encapsulation in nanoorganized microshells. *Nano Lett.* **1,** 125–128 (2001).
3. Gao, C., Donath, E., Möhwald, H. & Shen, J. Spontaneous deposition of water-soluble substances into microcapsules: phenomenon, mechanism, and application. *Angew. Chem. Int. Edn* **41,** 3789–3793 (2002).
4. Ibarz, G., Dähne, L., Donath, E. & Möhwald, H. Smart micro- and nanocontainers for storage, transport, and release. *Adv. Mater.* **13,** 1324–1327 (2001).
5. Sukhorukov, G. B., Antipov, A. A., Voigt, A., Donath, E. & Möhwald, H. pH-controlled macromolecule encapsulation in and release from polyelectrolyte multilayer nanocapsules. *Macromol. Rapid Commun.* **22,** 44–46 (2001).
6. Antipov, A. A., Sukhorukov, G. B. & Möhwald, H. Influence of the ionic strength on the polyelectrolyte multilayers' permeability. *Langmuir* **19,** 2444–2448 (2003).
7. Glinel, K., Sukhorukov, G. B., Möhwald, H., Khrenov, V. & Tauer, K. Thermalsensitive hollow capsules based on thermoresponsive polyelectrolytes. *Macromol. Chem. Phys.* **204,** 1784–1790 (2003).
8. Radt, B., Smith, T. A. & Caruso, F. Optically addressable nanostructured capsules. *Adv. Mater.* **16,** 2184–2189 (2004).
9. Zou, S., Hempenius, M. A., Schönherr, H. & Vancso, G. J. Force spectroscopy of individual stimulus-responsive poly(ferrocenyldimethylsilane) chains: towards a redox-driven macromolecular motor. *Macromol. Rapid Commun.* **27,** 103–108 (2006).
10. Zou, S., Korczagin, I., Hempenius, M. A., Schönherr, H. & Vancso, G. J. Single molecule force spectroscopy of smart poly(ferrocenylsilane) macromolecules: towards highly controlled redox-driven single chain motors. *Polymer* **47,** 2483–2492 (2006).
11. Kwon, I. C., Bae, Y. H. & Kim, S. W. Electrically credible polymer gel for controlled release of drugs. *Nature* **354,** 291–293 (1991).
12. Yerushalmi, R., Scherz, A., van der Boom, M. E. & Kraatz, H.-B. Stimuli responsive materials: new avenues toward smart organic devices. *J. Mater. Chem.* **15,** 4480–4487 (2005).
13. Pudelski, J. K. *et al.* Synthesis, characterization, and properties of high molecular weight poly(methylated ferrocenylsilanes) and their charge transfer polymer salts with tetracyanoethylene. *Macromolecules* **29,** 1894–1903 (1996).
14. Nguyen, M. T., Diaz, A. F., Dement'ev, V. V. & Pannell, K. H. High molecular weight poly(ferrocenediyl-silanes): synthesis and electrochemistry of $[-(C_5H_4)Fe(C_5H_4)SiR_2-]_n$, R = Me, Et, *n*-Bu, *n*-Hex. *Chem. Mater.* **5,** 1389–1394 (1993).
15. Arsenault, A. C., Miguez, H., Kitaev, V., Ozin, G. A. & Manners, I. A polychromic, fast response metallopolymer gel photonic crystal with solvent and redox tunability: a step towards Photonic Ink (P-Ink). *Adv. Mater.* **15,** 503–507 (2003).
16. Rulkens, R. *et al.* Linear oligo(ferrocenyldimethylsilanes) with between two and nine ferrocene units: electrochemical and structural models for poly(ferrocenylsilane) high polymers. *J. Am. Chem. Soc.* **118,** 12683–12695 (1996).
17. Péter, M. *et al.* Electrochemically induced morphology and volume changes in surface-grafted poly(ferrocenyldimethylsilane) monolayers. *Langmuir* **20,** 891–897 (2004).
18. Shi, W. *et al.* Single-chain elasticity of poly(ferrocenyldimethylsilane) and poly(ferrocenylmethylphenylsilane). *Macromolecules* **37,** 1839–1842 (2004).
19. Hempenius, M. A., Robins, N. S., Péter, M., Kooij, E. S. & Vancso, G. J. Water-soluble poly(ferrocenylsilanes) for supramolecular assemblies by layer-by-layer deposition. *Langmuir* **18,** 7629–7634 (2002).
20. Hempenius, M. A. & Vancso, G. J. Synthesis of polyanionic water-soluble poly(ferrocenylsilane). *Macromolecules* **35,** 2445–2447 (2002).
21. Hempenius, M. A., Brito, F. F. & Vancso, G. J. Synthesis and characterization of anionic and cationic poly(ferrocenylsilane) polyelectrolytes. *Macromolecules* **36,** 6683–6688 (2003).
22. Ginzburg, M. *et al.* Layer-by-layer self-assembly of organic-organometallic polymer electrostatic superlattices using poly(ferrocenylsilanes). *Langmuir* **16,** 9609–9614 (2000).
23. Decher, G. Fuzzy nanoassemblies: toward layered polymeric multicomposites. *Science* **277,** 1232–1237 (1997).

24. Donath, E., Sukhorukov, G. B., Caruso, F., Davis, S. A. & Möhwald, H. Novel hollow polymer shells by colloid-templated assembly of polyelectrolytes. *Angew. Chem. Int. Edn* **37,** 2201–2205 (1998).
25. Caruso, F., Lichtenfeld, H., Donath, E. & Möhwald, H. Investigation of electrostatic interactions in polyelectrolyte multilayer films: binding of anionic fluorescent probes to layers assembled onto colloids. *Macromolecules* **32,** 2317–2328 (1999).
26. Antipov, A. A. *et al*. Carbonate microparticles for hollow polyelectrolyte capsules fabrication. *Colloids Surf. A* **224,** 175–183 (2003).
27. Zhu, H., Stein, E. W., Lu, Z., Lvov, Y. M. & McShane, M. J. Synthesis of size-controlled monodisperse manganese carbonate microparticles as templates for uniform polyelectrolyte microcapsule formation. *Chem. Mater.* **17,** 2323–2328 (2005).
28. Zhang, H. & Rühe, J. Polyelectrolyte multilayers on weak polyelectrolyte brushes. *Macromol. Rapid Commun.* **24,** 576–579 (2003).
29. Giannotti, M. I. *et al*. Stimulus responsive poly(ferrocenylsilanes): redox chemistry of iron in the main chain. *J. Inorg. Organom. Polym. Mater.* **15,** 527–540 (2005).

Acknowledgements

The authors are grateful to E. S. Kooij (University of Twente) for his help with the ellipsometry measurements on planar multilayer films and to A. Heilig for her help with the AFM measurements in the Max Planck Institute of Colloids and Interfaces, Golm. The University of Twente, the MESA$^+$ Institute for Nanotechnology of the University of Twente, the Dutch Science Foundation for Chemical Research NWO-CW and NanoImpuls, a Nanotechnology Program of the Ministry of Economic Affairs of the Netherlands, are acknowledged for financial support.
Correspondence and requests for materials should be addressed to G.J.V.
Supplementary Information accompanies this paper on www.nature.com/naturematerials.

Competing financial interests

The authors declare that they have no competing financial interests.